COBEM 2021 Florianópolis - Brasil
ABCM Associação Brasileira de Engenharia e Ciências Mecânicas
26th ABCM International Congress of Mechanical Engineering
November 22-26, 2021. Florianópolis, SC, Brazil

COB-2021-1080
HUMANOID WALKING FOR A ROBOT WITH CURVED FEET

Caroline Cristine Duarte da Silva
Marcos R. O. A. Maximo
Autonomous Computational Systems Lab (LAB-SCA), Aeronautics Institute of Technology - Praça Marechal Eduardo Gomes, 50 - Vila das Acácias, 12228-900, São José dos Campos- SP/Brazil
carolcds@ita.br
mmaximo@ita.br

Luiz Carlos Sandoval Góes
Mechanical Engineering Division, Aeronautics Institute of Technology - Praça Marechal Eduardo Gomes, 50 - Vila das Acácias, 12228-900- São José dos Campos - SP/Brasil
goes@ita.br

Abstract.
This paper proposes the development of an energy-saving walking strategy for a humanoid robot. Despite the human appearance, humanoids expend much more energy while walking than humans. To this end, we unite the center of mass (CoM) vertical oscillation with pre-defined trajectories in gait that assure the performance of the curved robotic foot. We were inspired by several biomechanical studies that show why human walking is energy efficient. For example, the curvature of the human foot provides a wheel-like bearing, which lowers the cost of walking. Our contribution is to adapt the gait, which contemplates the vertical oscillation of the center of mass (CoM) with a curved robotic foot. We extend the Preview Control of Zero-Moment Point technique to plan the CoM trajectory oscillation and calculate the ankle trajectories through polynomial expressions. Due to the many degrees of freedom of the humanoid robot, we apply the modified the 3D Linear Inverted Pendulum Model (3D-LIPM). We validate our simulated results by implementing the proposed control technique described above in our custom-made robot Chape. Our results showed a simulation of stable gait, encompassing human-like motions in a robot.

Keywords: *Humanoid Robot, MPC, Walking, Robotic Foot.*

1. INTRODUCTION

Mobile robotics has fascinated researchers for a long time. In this paper, we deal specifically with the walk of humanoid robots. Humanoids are interesting because they have a human-like appearance and can interact in our environment with human tools. However, in reality, their behavior is different from humans, especially from an energetic point of view, limiting the robot's use. This difference in behavior is one of the reasons for many research challenges.

For example, the walking of a state-of-the-art Asimo robot (Takenaka *et al.*, 2009) uses ten times more the energy then a human (Collins *et al.*, 2005). This difference occurs because robotic movements are complex from a control point of view due to non-linearity, under-actuation, and high dimensionality, all of which represent a challenge to the latest generation control techniques (Collins *et al.*, 2005).

For our walk to be stable, we use the usual humanoid concept of Zero Moment Point (ZMP). The ZMP references the point on the ground where the reaction forces must act to stabilize the biped mechanism, according to Vukobratović and Borovac (2004). When the ZMP is inside the support polygon, it coincides with the center of pressure (CoP). Therefore the robotic feet are significant because they are responsible for delimiting the support polygon; the ZMP must be inside the support polygon.

For the mathematical model of a humanoid, due to the many degrees of freedom, we apply a modified version of the 3D Linear Inverted Pendulum (3D-LIPM) model, used by Kajita *et al.* (2001) to obtain the trajectory of the CoM. Subsequently, inverse kinematics (IK) finds the angles of all robotic joints.

For the control of the walk, we extend the Preview Control of Zero-Moment Point technique, which is a semi-analytical method of bipedal walk control based on Model Predictive Control (MPC) (Kajita *et al.*, 2003). This technique is present in the state-of-the-art works, in addition to being implemented in several humanoids (Yi *et al.*, 2016).

In Silva *et al.* (2019), we applied the MPC technique using modified 3D-LIPM, as we varied the height of the CoM during the march of the humanoid robot Darwin OP2. We used a high fidelity simulator, in this case Gazebo (Koenig and

Howard, 2004), and we noticed a decrease in energy cost due to the vertical oscillation of the CoM. This paper intends to reapply the CoM vertical oscillation procedure with the MPC for a curved foot robot. We propose this to a low-cost humanoid robot designed by the Autonomous Computational Systems Lab (LAB-SCA), the Chape (Tonaco *et al.*, 2019).

In the literature, the current stage of development of robotic feet addresses different aspects, from the geometric shape to flexible materials for damping. Choi *et al.* (2016) introduced a toe mechanism with variable stiffness using a leaf spring and rubber ball in series, and pressure sensors. A prototype of these feet were used to validated the mechanism with experimental results. Leu *et al.* (2017) propose a foot prototype formed with two curved blades, in which the magnitude and location of the ground reaction force is used to calibrate the force sensors on the robot's foot. Conversely, the experiment summarizes in a single step of a single robotic leg.

ERNIE is a biped planar walking robot with a curved foot, controlled by HZD (Hybrid Zero Dynamics), with walking aided by a shaft, i.e., ERNIE does not stay upright by itself. Several simulations and experiments with different foot radii and ankle offsets (the location of the center of curvature) demonstrated that the large foot radius and no ankle offset strategy produces the most efficient gait (Martin *et al.*, 2014).

Another way to soften the impact is the elevation of the heel and toes during the walk. Seung-Joon and Lee (2016) present a locomotion controller that lifts the heel and toes during the gait, overcoming the kinematic restrictions. This model provides the support, helping the robot cross uneven terrain. Realistic simulations were performed on the humanoid robots THOR-RD and DARwIn-OP.

Our inspiration for changing Chape's feet came from Biomechanics literature, in that the trajectory and shape of the human foot influence the energy expenditure of walking. By analyzing the motion of a wheel, Adamczyk *et al.* (2006) examined the energy cost of walking for different foot curves, they measured the work and the metabolic rate for the redirection of the CoM during the gait in 10 individuals walking with different boot curvatures.

Additionally, Adamczyk and Kuo (2013) develop a dynamic walking model that predicts the energetic effects by changing the foot length and the foot radius, performing experiments on eight human individuals with the device designed in Adamczyk *et al.* (2006).

For Chape's foot, we propose a geometry consisting of three parts: a cylindrical sector corresponding to the heel, a parallelepiped for the sole, and another cylindrical sector representing the toes. The idea of this format is that the transition between the sectors that form the robotic foot should be smooth so that there are no discontinuities during elevation or inclination of the feet during changes in the phases of gait.

Our contribution is a new walking method that calculates feet's trajectory through polynomial expressions to find the joint positions of a fully actuated robot. Our robot combines CoM planning using modified MPC to allow the oscillation vertical of the CoM.

The remainder of this work is organized as follows. Section 2 derives a mathematical model for the robot dynamics. Section 3 presents the model of control based on MPC with constraints. Section 4 determines the predefined trajectories for the CoM oscillation and the ankles. Section 5 presents the simulation linear time-varying. Section 6 presents the simulation results that validate our approach. Finally, Section 7 concludes the paper and proposes future works.

2. MATHEMATICAL MODEL

A standard mathematical model used in literature to describe the walking dynamics of a humanoid robot is the LIPM model. In this work, we modified the final ZMP equation described in S. Kajita (2013), we make this modification to have a linear time-varying system since the height of the CoM is prescribed.

$$p_x = x - \frac{z}{\ddot{z} + g}\ddot{x}, \tag{1}$$

$$p_y = y - \frac{z}{\ddot{z} + g}\ddot{y}, \tag{2}$$

where g is the acceleration of gravity; p_x is the ZMP in the x direction; x is the CoM in the x direction; p_y is the ZMP in the y direction; z is height of the CoM; y is the CoM in the y direction.

For conciseness, a derivation only for x coordinates will be presented, as extending it to y coordinates is straightforward. In state-space, we obtain the following form:

$$\frac{d}{dt}\begin{bmatrix} x \\ \dot{x} \\ \ddot{x} \end{bmatrix} = \begin{bmatrix} 0 & 1 & 0 \\ 0 & 0 & 1 \\ 0 & 0 & 0 \end{bmatrix}\begin{bmatrix} x \\ \dot{x} \\ \ddot{x} \end{bmatrix} + \begin{bmatrix} 0 \\ 0 \\ 1 \end{bmatrix} u, \tag{3}$$

$$p_x = \begin{bmatrix} 1 & 0 & \dfrac{-z}{\ddot{z}+g} \end{bmatrix} \begin{bmatrix} x \\ \dot{x} \\ \ddot{x} \end{bmatrix}, \tag{4}$$

where $\begin{bmatrix} x & \dot{x} & \ddot{x} \end{bmatrix}^T \in \mathbb{R}^{3\times 1}$ is the state vector in the x direction; u again is the control variable.

The output variable is p_x. The robot is able to directly control the jerk (i.e., the derivative of acceleration), this assumption is common in humanoid robotics (Kajita *et al.*, 2003). Finally the variables available for feedback are the state variables.

Assuming zero order hold over a duration time T, we obtain a discretized state space model in both directions as follows:

$$\mathbf{X}[k+1] = \begin{bmatrix} 1 & T & T^2/2 \\ 0 & 1 & T \\ 0 & 0 & 1 \end{bmatrix} \mathbf{X}[k] + \begin{bmatrix} T^3/6 \\ T^2/2 \\ T \end{bmatrix} u[k], \tag{5}$$

where $\mathbf{X}[k] = [x[k]\ \dot{x}[k]\ \ddot{x}[k]]^T$, while the output is given by

$$Z[k] = \begin{bmatrix} 1 & 0 & -\dfrac{z[k]}{\ddot{z}[k]+g} \end{bmatrix} \mathbf{X}[k], \tag{6}$$

The discrete matrices A, B and C are

$$A = \begin{bmatrix} 1 & T & T^2/2 \\ 0 & 1 & T \\ 0 & 0 & 1 \end{bmatrix}, \tag{7}$$

$$B = \begin{bmatrix} T^3/6 \\ T^2/2 \\ T \end{bmatrix}, \tag{8}$$

$$C = \begin{bmatrix} 1 & 0 & -\dfrac{z[k]}{\ddot{z}[k]+g} \end{bmatrix}, \tag{9}$$

3. MODEL PREDICTIVE CONTROLLER

The control task consists of making the ZMP follow a predefined reference in the x direction and the y, respecting the area that comprises the foot size limit. Therefore, the system has only output constraints.

As previously stated, the system is linear time-varying, using a discrete space model for both directions, both of which are SISO type systems. The formulation of the cost function depends on the predicted output ($\hat{\mathbf{Z}}$) and the predicted control signal ($\hat{\mathbf{u}}$).

$$J(\hat{\mathbf{Z}}, \hat{\mathbf{u}}) = (\hat{\mathbf{Z}} - \hat{\mathbf{Z}}_{\mathbf{ref}})^T (\hat{\mathbf{Z}} - \hat{\mathbf{Z}}_{\mathbf{ref}}) + \rho \hat{\mathbf{u}}^T \hat{\mathbf{u}}, \tag{10}$$

where $\hat{\mathbf{Z}} \in \mathbb{R}^{N\times 1}$, $\hat{\mathbf{u}} \in \mathbb{R}^{M\times 1}$ and $\hat{\mathbf{Z}}_{\mathbf{ref}} \in \mathbb{R}^{M\times 1}$ describes the variable reference, N is the prediction horizon, M is the control horizon, and ρ is the control weight. The prediction equation has the following format:

$$\hat{\mathbf{Z}} = H\hat{\mathbf{u}} + \mathbf{f}, \tag{11}$$

where $H \in \mathbb{R}^{N\times M}$ is the dynamic matrix (Maciejowski, 2002) and $\mathbf{f} \in \mathbb{R}^{N\times 1}$ is the free response vector (Maciejowski, 2002), which are given by

$$H = \begin{bmatrix} C[k+1|k]B & 0 & \dots & 0 \\ C[k+2|k]AB & C[k+2|k]B & \dots & 0 \\ \vdots & \vdots & \vdots & \vdots \\ C[k+N|k]A^{N-1}B & C[k+N|k]A^{N-2}B & \dots & C[k+N|k]B \end{bmatrix}, \tag{12}$$

$$\mathbf{f} = \begin{bmatrix} C[k+1|k]A \\ C[k+2|k]A^2 \\ \vdots \\ C[k+N|k]A^N \end{bmatrix} \mathbf{X}[k], \tag{13}$$

3.1 Constraints

The restrictions only apply to the output excursions. For conciseness, we will only present a derivation only for x coordinates, as extending it to y coordinates is straightforward.

$$\begin{bmatrix} H \\ -H \end{bmatrix} \hat{\mathbf{u}} \leq \begin{bmatrix} p_{x_{max}} - \mathbf{f} \\ \mathbf{f} - p_{x_{min}} \end{bmatrix} \tag{14}$$

where $p_{x_{min}} \in \mathbb{R}^{N\times 1}$ is the minimum ZMP values in the x direction and $p_{xmax} \in \mathbb{R}^{N\times 1}$ is the maximum ZMP values in the x direction.

To find the value of $\hat{\mathbf{u}}$ we used the solver for objective quadratic functions of MATLAB, "quadprog" with the "interior-point-convex" method

4. PREDEFINED TRAJECTORIES

4.1 Center of mass height variation

The model cannot be non-linear. Therefore, the calculation of the vertical displacement of the CoM must be predefined, making the model linear time-varying.

The choice of function considers the variation of height (z) of CoM in discrete-time. Equation (15) describes this function.

$$z[k] = a\cos(2\pi f t[k]) + b, \tag{15}$$

where a is the amplitude; f is the frequency; $t[k]$ is the discrte-time; b is the nominal height of the CoM.

4.2 Foot trajectory

In classical robotics literature (Khatib, 2008), path planning is a common technique. This technique also can be used to plan the joint's positions of humanoid robots. For example, for the foot to roll, it is necessary to predefine the trajectory of the ankle, as this motion is responsible for moving the contact points of the curved foot with the ground. In a fully actuated humanoid robot, the ankle joint is driven by a servomotor.

The geometry of our robotic foot is made up of three parts. First, we chose cylindrical sections for the heel and the toe. During the rolling movement, the curvature radius of the cylinder is always orthogonal to the contact point. Fig. 1 presents a profile of a robotic foot in the sagittal plane. We describe the geometrical parameters used to propose a trajectory that respects the foot bearing.

In Fig.1, r_{Toe} is the radius of the cylindrical sector corresponding to the toe; l_{Toe} is the length between the center of the cylindrical sector corresponding to the toe and the ankle joint; α_{Toe} is the angle between l_{Toe} and horizontal; r_{Heel} is the radius of the cylindrical sector corresponding to the heel; l_{Heel} is the length between the center of the cylindrical sector corresponding to the heel and the ankle; α_{Heel} is the angle between l_{Heel} and horizontal.

Because the space is three-dimensional, we propose an ankle trajectory in the three directions. However, before defining the ankle trajectory, we must consider that the gait cycle consists of two phases: double support (both feet are on the ground) and single support (one foot on the ground and one foot in swing). Therefore, we divide the time domain according to the time in which each phase occurs.

Then, θ is the angle the foot makes with the ground in sagittal plane. However, the angle θ varies in time because the foot moves. In Fig. 2.a, θ_{Toe} angle represents the value of θ at the moment the swing phase begins, i.e., the toe-off movement. In Fig. 2.b , θ_{Heel} angle represents the value of θ at the moment the swing phase ends, i.e., the heel strike movement.

Thereby, we were able to define the angles $\theta(\phi)$ of the foot, in the Eq. (16).

$$\begin{cases} \theta(\phi) = w_1\phi^3 + w_2\phi^2 + w_3\phi + w_4, \;\; if \;\; 0 \leq \phi < \phi_B, \\ \theta(\phi) = w_5\phi^3 + w_6\phi^2 + w_7\phi + w_8, \;\; if \;\; \phi_B \leq \phi \leq \phi_F, \\ \theta(\phi) = w_9\phi^3 + w_{10}\phi^2 + w_{11}\phi + w_{12}, \;\; if \;\; \phi > \phi_F, \end{cases} \tag{16}$$

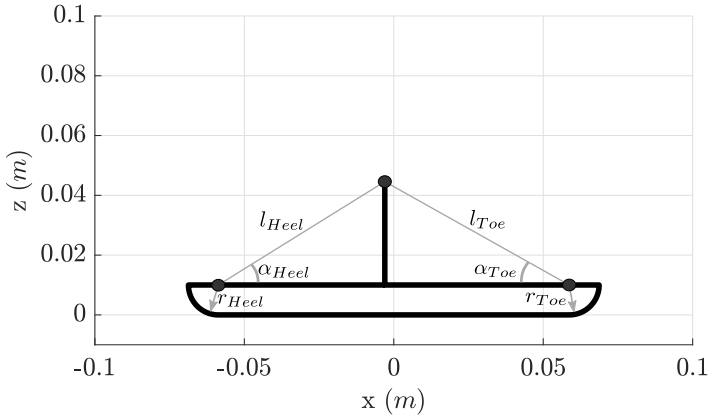

Figure 1: Geometric parameters of the curved foot are needed to simulate the humanoid walk.

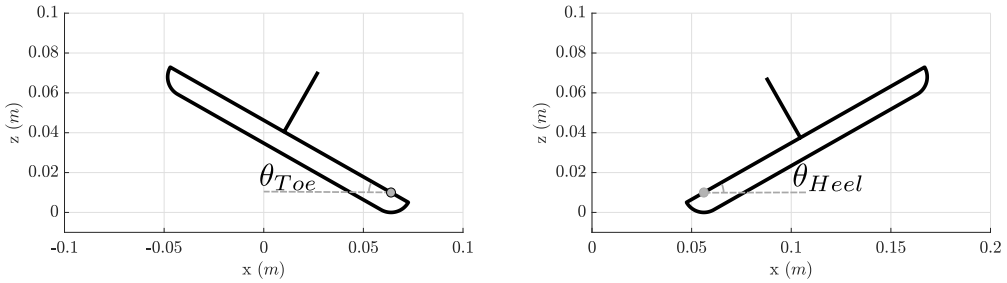

(a) The toe-off movement.

(b) The heel strike movement.

Figure 2: The swing phase begins and the swing phase ends, respectively.

where ϕ is the normalized time within a step; ϕ_B is the normalized time of the beginning of the single support phase; ϕ_F is the normalized time of the end the single support phase; w_1, w_2, w_3, ..., w_{12} are the cubic polynomial coefficients.

In Eq. (16), we propose to find $\theta(\phi)$ by interpolating cubic polynomials for the duration of each phase. We find the coefficients of the polynomials by solving a resulting linear system by applying the following conditions: θ_{Toe}, $\dot{\theta}_{Toe}$, θ_{Heel}, $\dot{\theta}_{Heel}$, $\theta(0)$, $\dot{\theta}(0)$, $\theta(1)$, $\dot{\theta}(1)$.

With this angle, we can define the ankle trajectory for each direction. To determine the path in z direction, we use Eq. (17). We observed that in the z direction, three curves form the trajectory. As the gait phase changes, the equation that governs the trajectory also changes.

$$\begin{cases} z(\phi) = r_{Toe} + l_{Toe} \mid \sin(\theta(\phi) + \alpha_{Toe}) \mid, \ \ if \ \ \phi < \phi_B, \\ z(\phi) = q_1\phi^4 + q_2\phi^3 + q_3\phi^2 + q_4\phi + q_5, \ \ if \ \ \phi_B \leq \phi \leq \phi_F, \quad , \\ z(\phi) = r_{Heel} + l_{Heel} \mid \sin(\theta(\phi) + \alpha_{Heel}) \mid, \ \ if \ \ \phi > \phi_F, \end{cases} \tag{17}$$

where ϕ is the normalized time within a step; ϕ_B is the normalized time of the beginning of the single support phase; ϕ_F is the normalized time of the end the single support phase; r_{Toe}, l_{Toe}, α_{Toe}, r_{Heel}, l_{Heel}, α_{Heel} are geometric foot parameters.; q_1, q_2, q_3, q_4, q_5 are the fourth degree polynomial coefficients. Again, we find the coefficients of the polynomials by solving a resulting linear system by applying the following conditions: $z(\theta(\phi_B))$, $\dot{z}(\theta(\phi_B))$, $z(\theta(\phi_F))$, $\dot{z}(\theta(\phi_F)$ and z$((\theta(\phi_F) + \theta(\phi_B))/2)$.

To define the path in x direction, we use Eq. (18). Again, three curves form the path. According to the fact that the gait phase changes, the equation that governs this trajectory also changes.

$$\begin{cases} x(\phi) = \lambda(\theta(\phi)) - l_{Toe}\cos(\theta(\phi) + \alpha_{Toe}), \ \ if \ \ \phi < \phi_B, \\ x(\phi) = q_6\phi^4 + q_7\phi^3 + q_8\phi^2 + q_9\phi + q_{10}, \ \ if \ \ \phi_B \leq \phi \leq \phi_F, \ \ , \\ x(\phi) = \lambda(\theta(\phi)) + l_{Heel}\cos(\theta(\phi) + \alpha_{Heel}), \ \ if \ \ \phi > \phi_F, \end{cases} \tag{18}$$

where ϕ is the normalized time within a step; ϕ_B is the normalized time of the beginning of the single support phase; ϕ_F is the normalized time of the end the single support phase; $\lambda(\theta(\phi))$ is the point of contact of the foot with the ground, in the x coordinate; q_6, q_7, q_8, q_9, q_{10} are the fourth degree polynomial coefficients. One more time, we find the coefficients of the polynomials by solving a resulting linear system by applying the following conditions: $x(\theta(\phi_B))$, $\dot{x}(\theta(\phi_B))$, $x(\theta(\phi_F))$, $\dot{x}(\theta(\phi_F)$ and $x((\theta(\phi_F) + \theta(\phi_B))/2)$.

In this paper in y direction, the path has only one parameter related to the separation between the feet.

$$y(\phi) = \delta, \tag{19}$$

where δ is a constant value.

5. SIMULATION

In this section, we present an overview of a simulation in MATLAB of the walking of a humanoid robot. First, we plan the CoM trajectory combined with polynomial expressions to determine the feet trajectories. Then, an inverse kinematics solver computes joint angles. In this paper, we used parameters for our humanoid robot, Chape. In Fig 3.a, we show our actual robot, and in Fig 3.b, we offer the functional diagram of our simulation that allows us to find the joint angles. Our code with the implemented simulation is available[1].

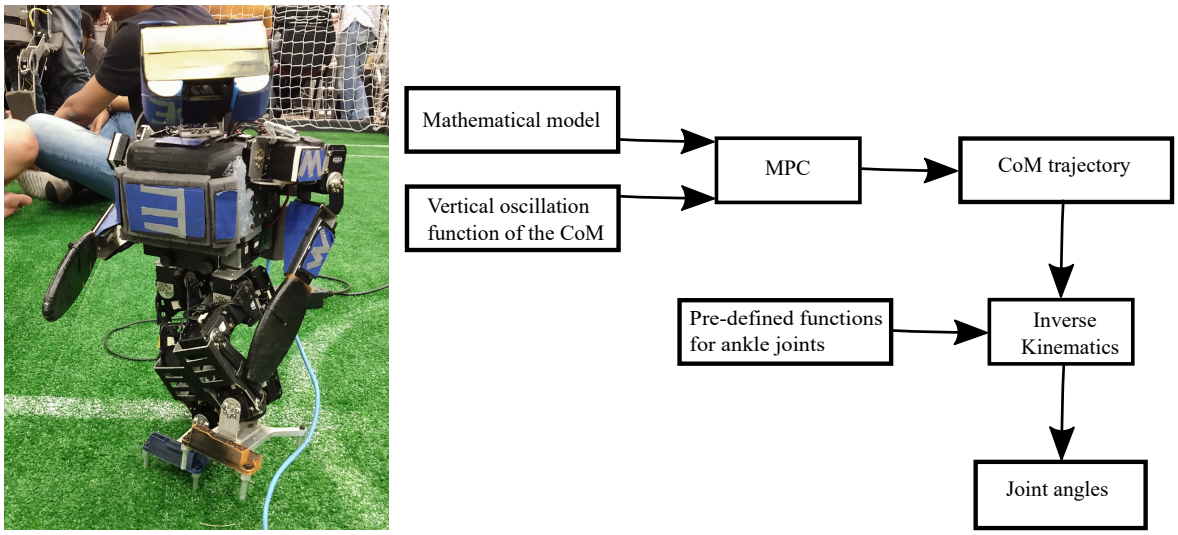

(a) Our real robot humanoid: Chape. (b) Diagram of how our simulation works.

Figure 3: Our physical robot and flowchart of our simulation.

5.1 Parameters for the model predictive control

Using MPC approach, in Tab. 1 describes the simulation parameters exposed in the Section 3. To choose the parameters of the function described in Eq. (15), we use our article Silva *et al.* (2019) for the frequency, where the robot's gait frequency is 2.5 Hz, for amplitude, we use the value of the radius of curvature of the proposed foot.

5.2 Kinematics of the rolling foot

Because the foot is a rigid body, we can define its trajectory through the ankle. For the curved foot to roll, we establish curves for the right and left ankle in Section 4. We chose $\theta_{Toe} = 25°$ and $\theta_{Heel} = -25°$. Figure 4.a illustrates the behavior of the right and left ankles in three-dimensional space. The blue and black curves correspond to the left and right ankle trajectories, respectively. Both curves have an oscillatory behavior and a cyclic repetition since the gait has a cyclical behavior.

[1] https://gitlab.com/itandroids/open-projects/humanoid-walking-with-curved-feet

Table 1: Simulation parameters for MPC.

Parameters for the MPC	**Value**
g, m/s^2	9.81
T, s	0.04
M	60
N	60
ρ	10^{-9}
Feet separation, m	0.1
Step duration, s	0.4
Velocity, m/s	0.2

Since in the y direction, the curves have a constant value, we can analyze ankle behaviors from the sagittal plane illustrated in Fig. 4.b. Thus, we can make two inferences about the walking behavior concerning the rolling of the foot. The first inference concerns the gap between the curves at the beginning of the trajectory in the x direction. The second inference concerns the shape of the curves. Three functions form each of the curves. This change between functions is evident because, in our walking, one foot can only swing when the other is completely flat on the floor.

In the transition between the double support phase for the swing phase, the foot that will swing makes a toe rolling motion. In the transition between the swing phase for the double support phase, the foot that ends the swing makes a heel rolling motion. The third inference concerns the gap in the z direction between the blue and black curves. When one curve reaches its maximum value, the other is at its minimum value.

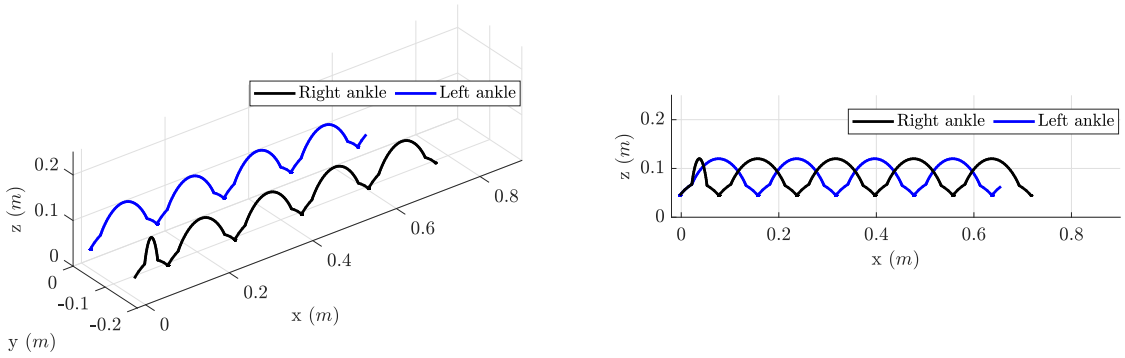

(a) Ankle trajectory in three-dimension space.

(b) Ankle trajectory in sagittal plane.

Figure 4: Ankle trajectories determined by polynomial expressions.

6. RESULTS

The reference signal of the system must follow the x direction and y direction, as seen in Maximo *et al.* (2017) for the desired ZMP. We opted for this approach because Maximo *et al.* (2017) propose a manipulation of reference ZMP for an energy-efficient walk using MPC.

For the step planner, we consider the time the robot is in double support and single support. Therefore, the total time of the simulation is 4 s. For better visualization, we represent only 11 steps in Fig. 5, the green curve represents the system output combination in the x direction and y direction, the red curve indicates the combination of the ZMP reference. The rectangles in black color are feet positions.

Still, in Fig. 5, the blue curve shows the CoM displacement combination of x direction and y direction. We notice a steady oscillatory behavior, which was expected since the walk is a cycle. The ZMP stays at the edge of the foot because we use a formulation that moves the ZMP during the step for better energy efficiency. Still, the ZMP remains within the boundaries of the supporting polygon.

Figure 6.a illustrates the behavior of the CoM, in the three-dimensional space, of the MATLAB model with vertical oscillation. The axes indicate the directions of the CoM. For a better view, Fig. 6.b shows the CoM behavior for each direction during the simulation time.

In Fig. 6.b, the blue curve corresponds to the displacement of the CoM in the x direction. Its value increases as time increases due to the forward mo vent of the robot. The red curve corresponds to the displacement of the CoM in

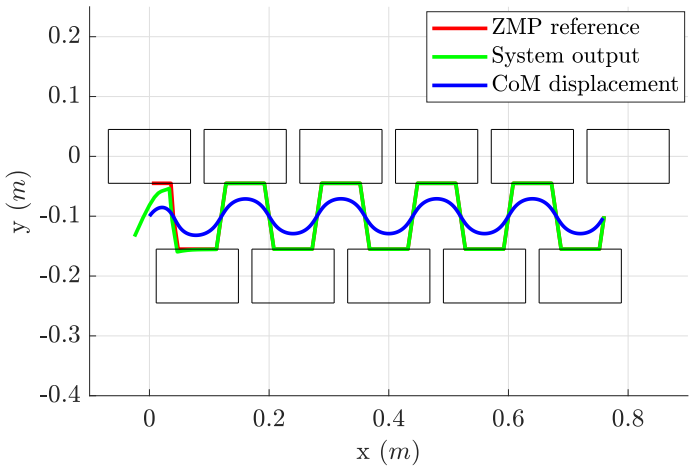

Figure 5: Walk simulation with feet positions, seen from the XY plane.

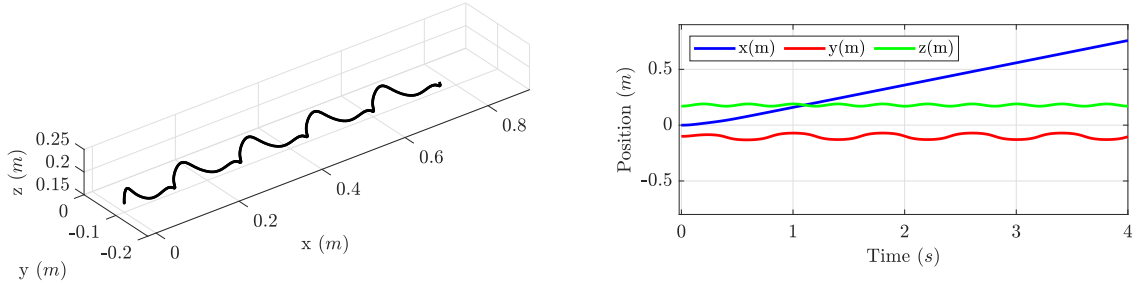

(a) CoM trajectory of MATLAB simulation in three-dimension space.

(b) CoM trajectory of MATLAB simulation in time.

Figure 6: CoM trajectory.

the y direction. It has a cyclical behavior due the walk having an oscillatory patter in the transverse plane. The green curve corresponds to the displacement of the CoM in the z direction. So again, we have a cyclical behavior, however we predefined the CoM oscillation in the z direction.

For better visualization of our simulation, Fig. 7 depicts only one step in the sagittal plane to describe what happens during one step in the gait. The blue and red colors represent the left and right legs, respectively. Moreover, we made a video[2] of the simulation, with a rate of 50 Hz. This video shows that when one foot enters or leaves the swing, the other is completely flat on the ground.

In Fig 7.a, the robot is double supported. In Fig 7.b, the right foot is almost finishing the toe roll movement, which means the right leg will swing. In Fig 7.c, the robot is in the swing phase, and the swing foot (right foot) is at its maximum height. Finally, in Fig 7.d, the robot is again in the double support phase, meaning the right foot is beginning the heel roll movement. Finally, in Fig 7.e, the right foot overtook the left foot. During the entire movement of the right leg, the left foot remains flat on the ground. However, the cycle is repeated in the next step, but with inverted roles, the left leg will swing, and the right foot will be flat on the ground. Therefore, alternating between swing foot and support foot, the robot moves.

7. CONCLUSION

We concluded that our gait proved to be stable, and our proposal to unite the trajectories that provide a robotic foot roll similar to a wheel left our robot with a walk more similar to humans. We combined these trajectories with CoM's

[2]https://www.youtube.com/watch?v=NB_q3UBvC44

vertical oscillation dynamics, and we believe we create a more energy-efficient walking method.

For future work, we intend to make our gait model omnidirectional. Furthermore, we expect to measure the energy used for the full gait, using all the robot dynamics in a realistic simulator, such as Gazebo. Finally, we intend to experiment with measuring battery usage. For this, we are considering the construction of the physical device of the curved foot because currently, the Chape's is flat, as shown in Fig 3.a.

It is essential to highlight that the walk proposed in this paper is not exclusive to our robot. This walking method can be adapted to other robots just by modifying the simulation parameters.

8. ACKNOWLEDGEMENTS

Caroline Silva acknowledges CAPES-Proex (number 88887.288287-2018-00), for financial support. Moreover, the authors would like to thank its sponsors: Altium, Intel, ITAEx, Mathworks, Metinjo, Micropress, Polimold, Rapid, Solidworks, ST Microelectronics, TFG, and Virtual Pyxis.

9. REFERENCES

Adamczyk, P.G., Collins, S.H. and Kuo, A.D., 2006. "The advantages of a rolling foot in human walking". *The Journal of Experimental Biology*, Vol. 209, pp. 3953–3963.

Adamczyk, P.G. and Kuo, A.D., 2013. "Mechanical and energetic consequences of rolling foot shape in human walking". *The Journal of Experimental Biology*, Vol. 216, pp. 2722–2731.

Choi, W., Medrano-Cerda, G.A., Caldwell, D.G. and Tsagarakis, N.G., 2016. "Design of a Variable Compliant Humanoid Foot with a New Toe Mechanism". In *Proc. Int. Conf. Robotics and Automation*. Estocolmo, Suécia,, pp. 642 – 647.

Collins, S.H., Ruina, A., Tedrake, R. and Wisse, M., 2005. "Efficient bipedal robots based on passive-dynamic walkers". *Science*, Vol. 307, pp. 1082 – 1085.

Kajita, S., Kanehiro, F., Kaneko, K., Fujiwara, K., Harada, K., Yokoi, K. and Hirukawa, H., 2003. "Biped walking pattern generation by using preview control of zero-moment point". In *International Conference on Robotics and Automation*. Vol. 2, pp. 1620–1626.

Kajita, S., Kanehiro, F., Kaneko, K., Yokoi, K. and Hirukawa, H., 2001. "The 3D Linear Inverted Pendulum Mode: A simple modeling for a biped walking pattern generation". In *Proc. Int. Conf. Intelligent Robots and Systems*. Maui, EUA, pp. 239 – 246.

Khatib, S., 2008. *Springer Handbooks of Robotics*. Springer, Berlin.

Koenig, N. and Howard, A., 2004. "Design and use paradigms for gazebo, an open-source multi-robot simulator". In *2004 IEEE/RSJ International Conference on Intelligent Robots and Systems (IROS) (IEEE Cat. No.04CH37566)*. Vol. 3, pp. 2149–2154 vol.3. doi:10.1109/IROS.2004.1389727.

Leu, J.E., Chen, Y.H., Liu, S.T. and Shih, W.P., 2017. "Development of a Humanoid Robot Foot with Distributive Force Sensors". In *Proc. Int. Conf. Control, Automation and Robotics*. Nagoya, Japão,, pp. 134 – 137.

Maciejowski, J.M., 2002. *Predictive Control with Constraints*. Prentice Hall, New York.

Martin, A.E., Post, D.C. and Schmiedeler, J.P., 2014. "The effects of foot geometric properties on the gait of planar bipeds walking under hzd-based control". *The International Journal of Robotics Research*, Vol. 33, No. 12, pp. 1530–1543. doi:10.1177/0278364914532391.

Maximo, M.R.O.A., Ribeiro, C.H.C. and Afonso, R.J.M., 2017. " Reference ZMP Manipulation for Energetic and Computationally Eficient Walking Using ZMP Preview Control". In *XIII Simpósio Brasileiro de Automação Inteligente*. Porto Alegre, Brasil,.

S. Kajita, H. Hirukawa, K.H.K.Y., 2013. *Introduction to Humanoid Robotics*. Springer, London.

Seung-Joon and Lee, D.D., 2016. "Heel and Toe Lifting Walk Controller for Resource Constrained Humanoid Robots". In *Proc. Int. Conf. Intelligent Robots and Systems*. Daejeon, Coréia,, pp. 5452 – 5458.

Silva, C.C.D., Maximo, M.R.O.A. and Góes, L.C.S., 2019. " Height Varying Humanoid Robot Walking through Model Predictive Control". In *2019 Latin American Robotics Symposium (LARS)*. Rio Grande, Brazilian,.

Takenaka, T., Matsumoto, T. and Yoshiike, T., 2009. "Real Time Motion Generation and Control for Biped Robot -1st Report: Walking Gait Pattern Generation". In *Proc. Int. Conf. Intelligent Robots and Systems*. St. Louis, EUA, pp. 1084 – 1091.

Tonaco, T.R.O., Vacarini, D., Silva, C.C.D., Maximo, M.R.O.A. and Arbelo, M.A., 2019. " Humanoid Robot Leg Design". In *25th International Congress of Mechanical Engineering*. Uberlândia, Brazilian,.

Vukobratović, M. and Borovac, B., 2004. "Zero-Moment Point – Thirty Five Years of Its Life". *Int. J. Humanoid Robots*.

Yi, S.J., McGill, S., Hong, D. and Lee, D., 2016. "Hierarchical motion control for a team of humanoid soccer robots". *International Journal of Advanced Robotic Systems*, Vol. 13.

10. RESPONSIBILITY NOTICE

The authors are solely responsible for the printed material included in this paper.

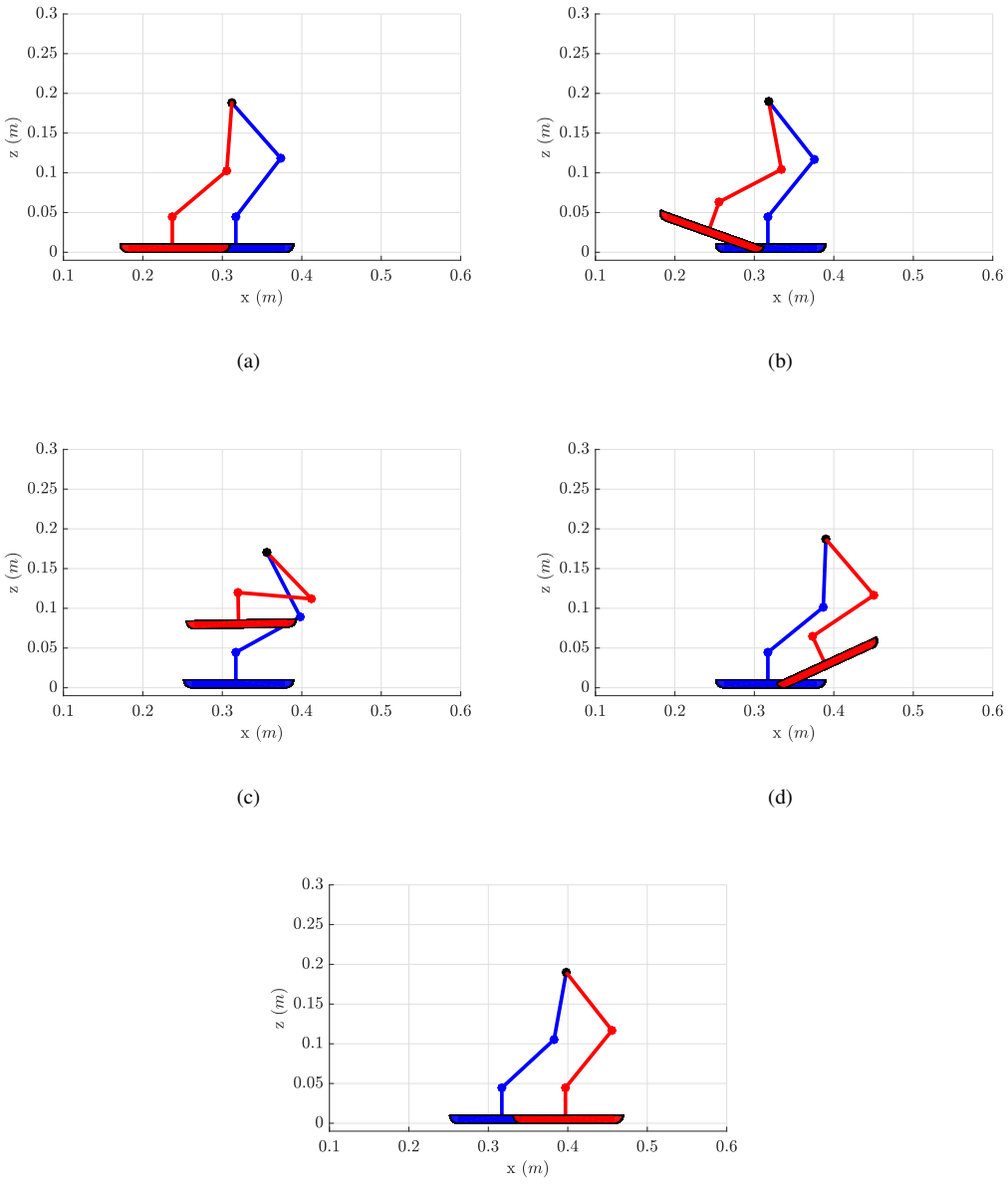

(a) (b)

(c) (d)

(e)

Figure 7: The walking with curved foot.